Cell Death and Differentiation (2009) 16, 298–311

www.nature.com/cdd

The tumor suppressor protein PML controls apoptosis induced by the HIV-1 envelope

J-L Perfettini[1,9], R Nardacci[2,9], C Séror[1], M Bourouba[1], F Subra[3], L Gros[3], G Manic[1], A Amendola[2], P Masdehors[4], F Rosselli[5], DM Ojcius[6], C Auclair[3], H de Thé[7], M-L Gougeon[4], M Piacentini[2,8,10] and G Kroemer*[,1,10]

Promyelomonocytic leukemia (PML) is a prominent oncosuppressor whose inactivation is involved in the pathogenesis of hematological and epithelial cancers. Here, we report that PML aggregated in nuclear bodies in syncytia elicited by the envelope glycoprotein complex (Env) of human immunodeficiency virus-1 (HIV-1) *in vitro*. PML aggregation occurred after the fusion of nuclei (karyogamy) within syncytia but before the apoptotic program was activated. The aggregation of PML was detectable in syncytia present in the brain or lymph nodes from patients with HIV-1 infection, as well as in a fraction of blood leukocytes, correlating with viral status. Using a range of specific inhibitors of PML (the oncogenic PML/RARα fusion product or specific small interfering RNAs), we demonstrated that, in Env-elicited syncytia, PML was required for activating phosphorylation of ataxia telangiectasia mutated (ATM), which colocalized with PML in nuclear bodies, in a molecular complex that also involved topoisomerase IIβ-binding protein 1. PML knockdown thus inhibited the ATM-dependent DNA damage response that culminates in the activation of p53, p53-dependent transcription of pro-apoptotic genes and cell death. Infection of CD4-expressing cells with HIV-1 also induced syncytial apoptosis, which could be suppressed by inhibiting PML. Altogether, these data indicate that PML activation is a critical early event that participates in the apoptotic demise of HIV-1-elicited syncytia.
Cell Death and Differentiation (2009) **16,** 298–311; doi:10.1038/cdd.2008.158; published online 21 November 2008

Human immunodeficiency virus (HIV), the causative agent of acquired immunodeficiency syndrome (AIDS), triggers T-cell depletion through apoptosis.[1–3] One particular – and poorly understood – mechanism by which HIV triggers host cell apoptosis is to induce the fusion between infected cells (which carry the HIV envelope (Env) glycoprotein complex) and uninfected cells (which carry the Env receptor CD4 and a coreceptor such as CXCR4 or CCR5).[4,5] As a result of cell-to-cell fusion (cytogamy), the cytoplasma of distinct cells is mixed and a syncytium is formed. After a latency, the nuclei contained in the common cytoplasm also fuse among each other and hence undergo karyogamy.[6,7] Then, a complex signal transduction cascade is activated that ultimately activates the mitochondrial pathway of apoptosis.[4,8–10] The importance of syncytial apoptosis in AIDS pathogenesis is controversial. However, a positive correlation between $CD4^+$ T-cell decline and infection by syncytium-inducing HIV-1 variants or orthologs has been established *in vivo*, in monkeys,[11] humanized SCID mice[12] and patients with AIDS.[13] Moreover, the so-called 'multinuclear giant cells', which are syncytia, accumulate in the cerebral cortex of patients with HIV-1-associated encephalopathy (HAE). The histopathological detection of such syncytia is pathognonomic for HAE,[14] meaning that their presence in frontal brain section is the sole criterion for the diagnosis of neuro-AIDS.

Karyogamy, the first step that leads to apoptotic demise of syncytia,[4,6] requires the cyclin-dependent kinase-1 (CDK1)-

[1]INSERM U848, Institut Gustave Roussy, Université Paris Sud, Paris 11, 39 rue Camille-Desmoulins, F-94805 Villejuif, France; [2]National Institute for Infectious Diseases 'Lazzaro Spallanzani', Via Portuense 292, 00149 Rome, Italy; [3]CNRS UMR 8113 LBPA, Ecole Normale Supérieure de Cachan, 61 avenue du Président Wilson, 94230 Cachan, France; [4]Antiviral Immunity, Biotherapy and Vaccine Unit, Department of Infection and Epidemiology, Institut Pasteur, 28 rue du Dr. Roux, 75724 Paris Cedex 15, France; [5]CNRS FRE2939, Institut Gustave Roussy, Université Paris Sud, Paris 11, 39 rue Camille-Desmoulins, F-94805 Villejuif, France; [6]School of Natural Sciences, University of California, Merced, CA, USA; [7]CNRS UPR9051, Université de Paris VII, Hôpital St. Louis, 1 avenue Claude Vellefaux, 75475 Paris Cedex 10, France and [8]Department of Biology, University of Rome 'Tor Vergata', Via della Ricerca Scientifica 1, 00173 Rome, Italy
*Corresponding author: G Kroemer, INSERM U848, Institut Gustave Roussy, Université Paris Sud, Paris 11, Pavillon de Recherche 1, 39, rue Camille-Desmoulins, F-94805 Villejuif, France. Tel: +33 1 42 11 60 46; Fax: +33 1 42 11 60 47; E-mail: kroemer@igr.fr
[9]These authors contributed equally to this paper
[10]These authors share senior coauthorship
Keywords: AIDS; apoptosis; ATM; envelope; p53; TopBP1
Abbreviations: AIDS, acquired immunodeficiency syndrome; ATM, ataxia telangiectasia mutated; ATMS1981P, ATM phosphorylated on serine 1981; Cdk1, cyclin-dependent kinase 1; Cyt *c*, cytochrome *c*; DN, dominant negative; Env, envelope glycoprotein complex; GAPDH, glyceraldehyde phosphate dehydrogenase; GFP, green fluorescent protein; HAART, highly active antiretroviral therapy; γ-H2AX, phosphorylated histone 2AX; HAE, HIV-1-associated encephalitis; HIV-1, human immunodeficiency virus-1; HU, hydroxyurea; IKSR, inhibitor of NF-kB super repressor; KG, karyogamy; MAPK, mitogen activated protein kinase; MKK, MAPK kinase; MKK3/6 S189/207P, MKK3 with phosphorylated serine 189 and/or MKK6 with phosphorylated serine 207; MOI, multiplicity of infection; NBS1, Nijmegen breakage syndrome 1; p38T180/Y182P, p38 with phosphorylated threonine 180 and tyrosine 182; p53S15P, p53 with phosphorylated serine 15; p53S46P, p53 with phosphorylated serine 46; PEG, polyethyleneglycol; PBMCs, peripheral blood mononuclear cells; PML, promyelomonocytic leukemia; PML/RARα, fusion protein between PML and retinoic acid receptor-α; pre-KG, pre-karyogamy; RARα, retinoic acid receptor-α; p53-iGFP, p53-inducible green fluorescent protein; SC, single cell; siRNA, small interfering RNA; SUMO-1, small ubiquitin-like modifier 1;Syn.,syncytia; UV-C, ultraviolet C light; TopBP1, topoisomerase IIβ-binding protein 1; VP16, etoposide; VSV, vesicular stomatitis virus; WT, wild type; Z-VAD-fmk, *N*-benzyloxycarbonyl-Val-Ala-Asp-fluoromethylketone
Received 17.4.08; revised 29.8.08; accepted 23.9.08; Edited by G Melino; published online 21.11.08

mediated dissolution of the nuclear envelope and is accompanied by the mTOR-mediated phosphorylation of p53 on serine 15 (p53S15P).[6,15] However, the sole phosphorylation of p53 on serine 15 is not sufficient to induce syncytial apoptosis, which requires a second phosphorylation of p53 on serine 46 (p53S46P).[8] As a result of karyogamy among non-synchronized nuclei, HIV-1-elicited syncytia activate a DNA damage response involving typical DNA damage foci that contain phosphorylated histone histone 2AX (γ-H2AX) as well as the H2AX-phosphorylating kinase ataxia telangiectasia mutated (ATM).[16] The activation of ATM (which is accompanied by its phosphorylation on serine 1981 (ATMS1981P)) ultimately triggers the activating phosphorylation of p38 mitogen-associated protein kinase (MAPK), which finally phosphorylates p53 on serine 46.[16] Then, p53 transactivates pro-apoptotic proteins such as Puma, thereby triggering mitochondrial membrane permeabilization, cytochrome *c* (Cyt *c*) release and caspase activation.[9] The pathway delineated above (ATM→p38 MAPK→p53→Puma) has been deciphered in syncytia generated by the coculture of *Env*-transfected and *CD4*-expressing cells,[9] and the activating phosphorylation of ATM, p38 MAPK and p53, as well as the overexpression of PUMA, has been detected in syncytia contained in the lymph nodes or brains from HIV-1-infected donors.[8,9,16,17]

The mechanisms through which ATM is activated within DNA damage foci of karyogamic nuclei are elusive. One particular nuclear substructure is formed by the so-called promyelomonocytic leukemia (PML) nuclear bodies (PML-NBs).[18] PML-NBs are defined by the presence of a protein called PML, a prominent oncosuppressor that is inactivated in some leukemias[19,20] and non-small

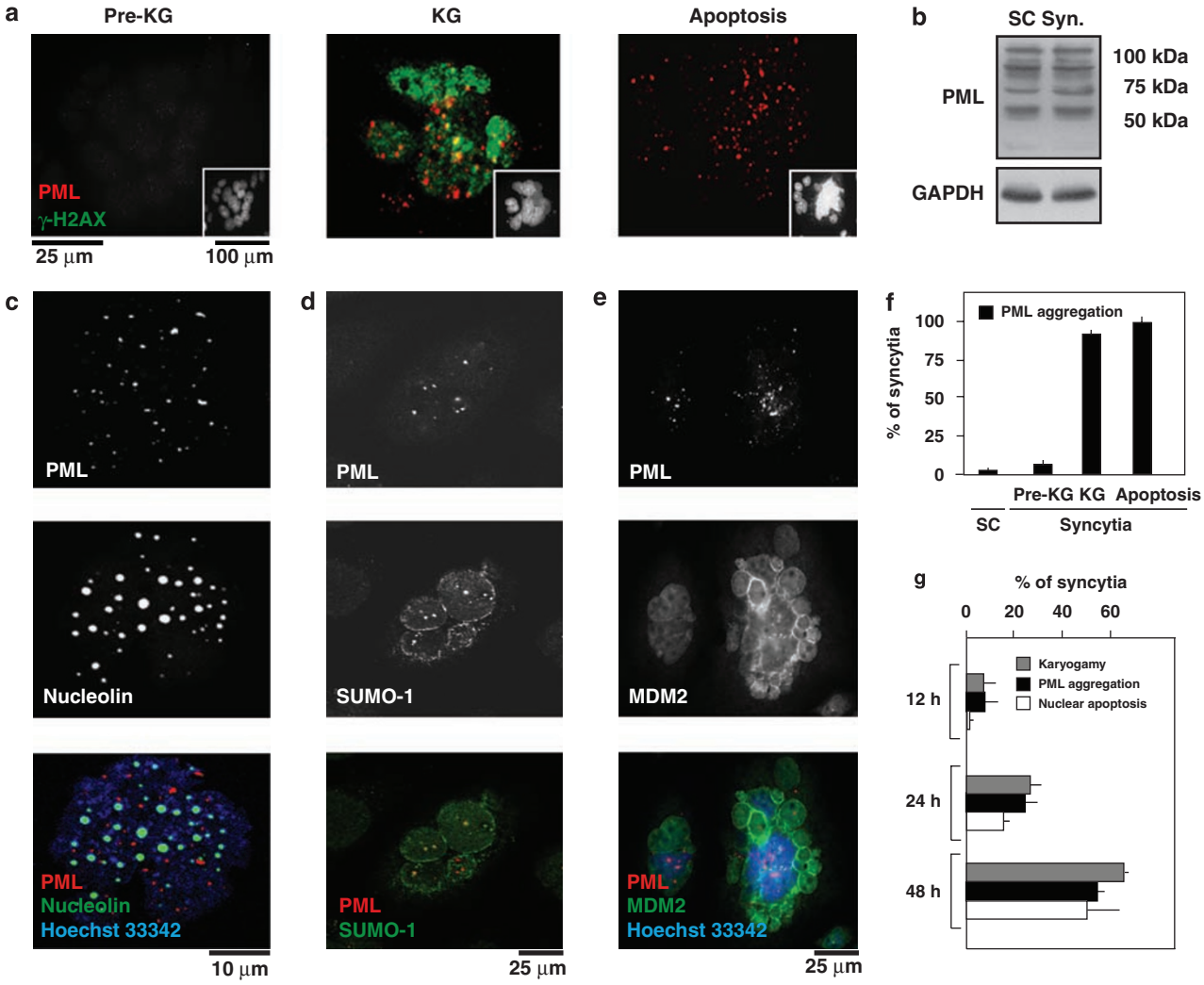

Figure 1 PML aggregation in karyogamic syncytia elicited by HIV-1 Env. (**a**) PML aggregation and histone H2AX phosphorylation. Syncytia were generated by coculture of HeLa CD4 and HeLa Env cells (36 h), followed by immunofluorescence double staining of PML and γ-H2AX. Representative pre-karyogamic (pre-KG), karyogamic (KG) and apoptotic cells are shown. The inserts depict the staining with the chromatin-specific dye Hoechst 33342. (**b**) PML expression levels. Extemporaneous 1 : 1 mixtures of HeLa Env and HeLa CD4 single cells (SC) or syncytia (48 h, which are mixtures of pre-KG and KG cells) were subjected to immunoblot detection of PML. (**c**–**e**) Colocalization of PML with nucleolin and SUMO-1. Representative immunofluorescence pictures of karyogamic syncytia induced as in (**a**) are shown after staining with anti-PML, Hoechst 33342, nucleolin (**c**), SUMO-1 (**d**) or anti-MDM2 (**e**). (**f**) Quantitation of PML activation in distinct categories of syncytia, as determined in (**a**). (**g**) Time course of PML activation in syncytia, as determined by immunofluorescence stainings with anti-PML (as in (**a**)) ($X \pm$ S.D., $n = 3$)

lung cancer.[19,21] The number and size of PML-NBs increase in response to soluble factors and cellular stress, which has led to the notion that PML-NBs are stress-responsive structures.[22] Indeed, PML-NBs are dynamic structures that favor the sequestration and release of DNA repair and checkpoint proteins, mediate their post-translational modifications and promote specific nuclear events in response to various cellular stresses including DNA damage.[18,23–25]

Here, we report that PML forms large aggregates within the karyogamic syncytia of Env-elicited syncytia *in vitro* and in HIV-1-infected individuals. We provide evidence that PML is placed on the apex of the phosphorylation cascade involving ATM, p38 MAPK and p53. Moreover, we show that PML is required for syncytial apoptosis.

Results

Pre-apoptotic aggregation of PML in karyogamic syncytia. HIV-1 Env induces the formation of syncytia when cells transfected with HIV-1LAI *Env* are cultured together with cells transfected with *CD4*. In this model, apoptosis occurs only in syncytia (but not in single cells (SCs)), after nuclear fusion (karyogamy) has occurred and affects approximately 50% of all syncytia after 48 h of coculture. Karyogamic (but not freshly formed (pre-karyogamic) syncytia nor SCs) exhibited the aggregation of PML protein in discrete nuclear bodies (Figure 1a) without that an increase in the abundance of PML protein would be detectable by immmunoblot (Figure 1b). Both normal and syncytial PML aggregated in a non-nucleolar pattern

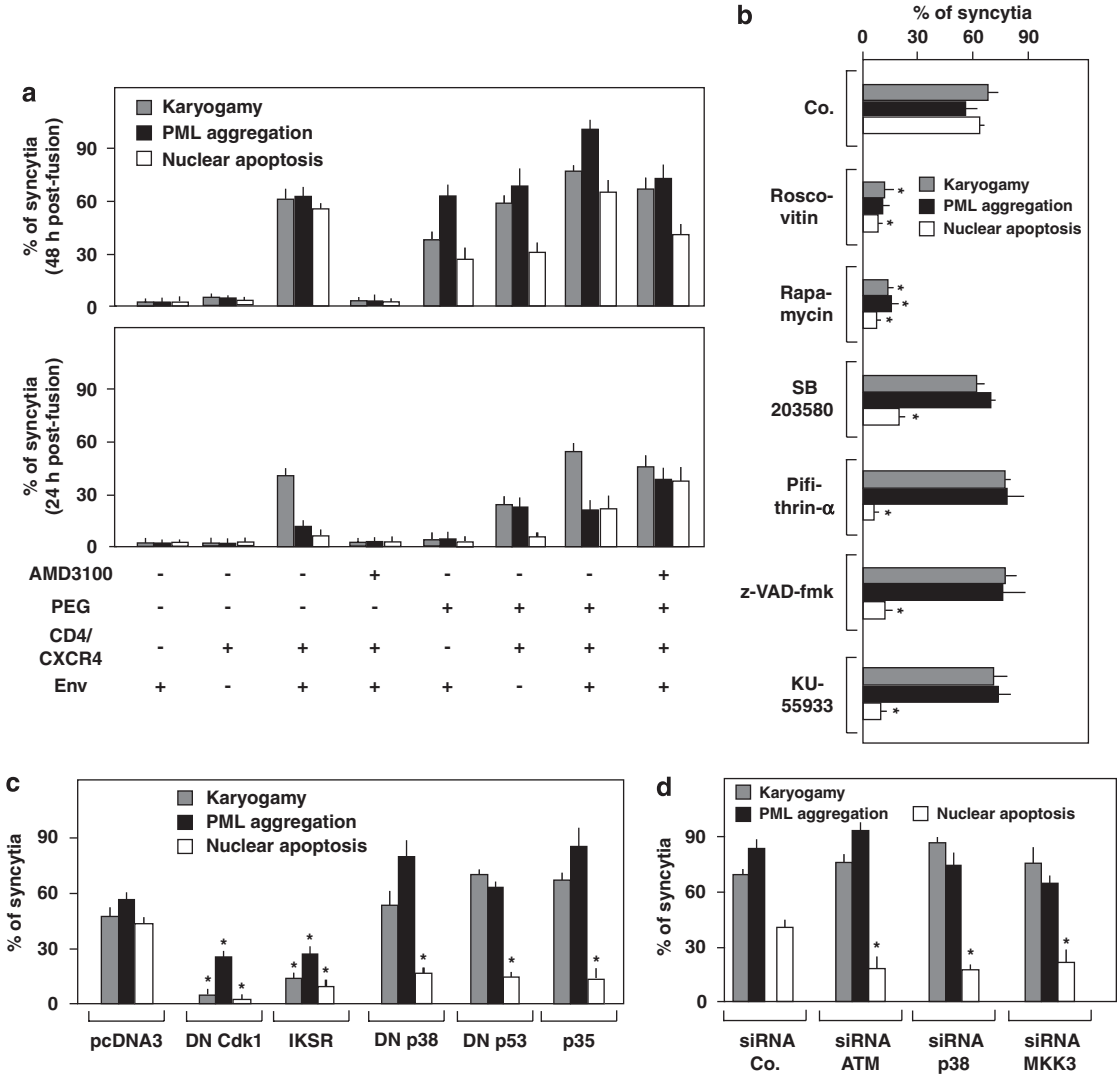

Figure 2 PML aggregation occurs as a consequence of karyogamy but before apoptosis. (**a**) Role of cell fusion in PML activation. Single cell (SC) or HeLa Env/HeLa CD4 cocultures were performed as in (**a**), in the absence or presence of the fusion inhibitor AMD3100. Alternatively, HeLa Env and HeLa CD4 cells were fused using polyethylene glycol (PEG), either separately or in mixed cultures, in the absence or presence of AMD3100. One day after fusion, karyogamy, nuclear apoptosis and PML aggregation were determined by immunofluorescence microscopy. (**b**–**d**) Modulation of PML aggregation by various inhibitors of karyogamy and apoptotic signaling. HeLa CD4 and HeLa Env cells were left untransfected (**b**) or were transfected with a series of control vectors and dominant-negative (DN) constructs 24 h before fusion (**c**) or with specific siRNAs 36 h before fusion (**d**) and then were cocultured for another 36 h. Finally, the cells were subjected to immunofluorescence microscopy for the detection of karyogamy, apoptosis (nuclear chromatin condensation) and PML aggregation. Results are shown as means ± S.D. of four independent experiments. Asterisks indicate significant ($P<0.01$, Student's *t*-test) effects

(Figure 1c) and colocalized with the small ubiquitin-like modifier-1 (SUMO-1) (Figure 1d, Supplementary Figure 1) and DAXX proteins (data not shown) but not with MDM2 (Figure 1e, Supplementary Table 1). The constant colocalization between SUMO-1 and PML before and after syncytium formation (Supplementary Figure 1) and the absence of any shift in the electrophoretic mobility of the different PML proteins (Figure 1b) suggest that changes in sumoylation likewise are not responsible for the aggregation of PML. Morphometric analyses of confocal immunofluorescence microphotographs revealed that karyogamic PML bodies ($0.75 \pm 0.20\,\mu$m, $X \pm$ S.E.M., $n = 103$) were significantly ($P < 0.001$, Student's t-test) larger in diameter than normal PML nuclear bodies ($0.41 \pm 0.09\,\mu$m, $n = 145$), as they are contained in normal unfused cells. Thus, the vast majority of PML bodies of SCs possess a diameter of $< 0.5\,\mu$m whereas $> 99\%$ of karyogamic syncytia bear PML bodies $> 0.5\,\mu$m. We refer to this phenomenon as 'PML aggregation'.

PML aggregation was abolished in the coculture system by the addition of a pharmacological inhibitor of Env-dependent

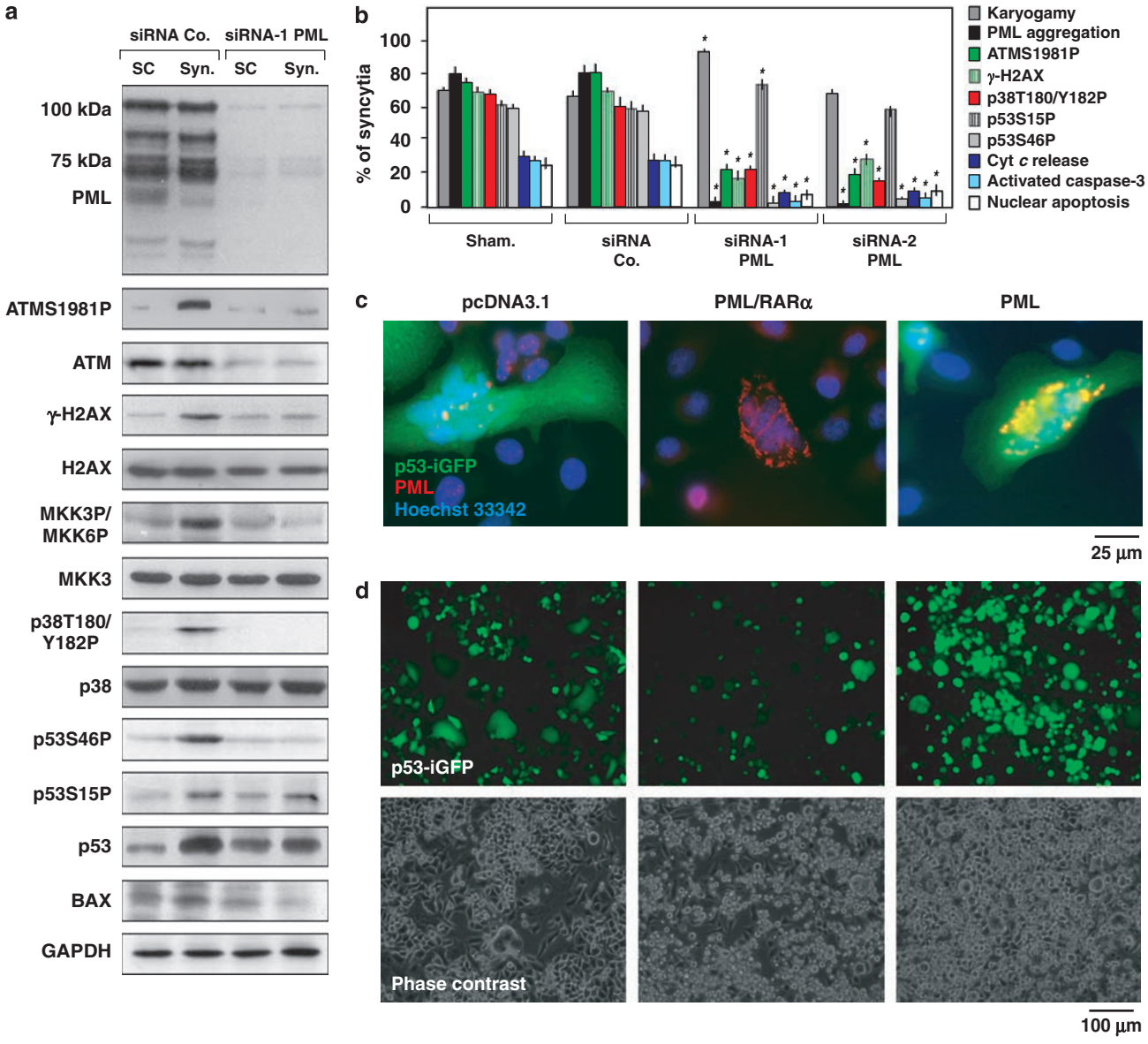

Figure 3 Suppression of the Env-elicited apoptotic signal transduction cascade by PML depletion or inhibition. (**a** and **b**) Effect of PML depletion. HeLa CD4 and HeLa Env cells were separately transfected with PML-specific siRNAs, and 36 h later, the cells were cocultured for a further 36 h, lysed and subjected to the immunochemical detection of the indicated proteins and phosphoproteins (**a**). Alternatively, the activation of pro-apoptotic signals was measured by immunofluorescence microscopy (**b**) ($X \pm$ S.D., $n = 5$). (**c**–**g**) Inhibition of Env-induced syncytial apoptosis by PML/RARα. HeLa CD4 and HeLa Env cells were separately transfected with a p53-inducible GFP construct, together with vector only (pcDNA3.1) or vectors driving the expression of PML, RARα or the PML/RARα fusion protein. Twenty-four hours later, the two cell lines were cocultured for 36 h and examined for PML aggregation and GFP expression. Representative syncytia are shown at high (**c**) and low (**b**) magnification. Moreover, GFP positivity ($X \pm$ S.D., $n = 3$) was quantitated by fluorescence microscopy (**e**) or immunoblot (**f**). In a separate series of experiments (**g**), the cells were transfected only with pcDNA3.1, PML or PML/RARα (24 h), then cocultured (36 h) and the frequency of cells exhibiting the indicated parameters was determined by immunofluorescence staining ($X \pm$ S.D., $n = 3$). Asterisks indicate significant ($P < 0.001$) effects

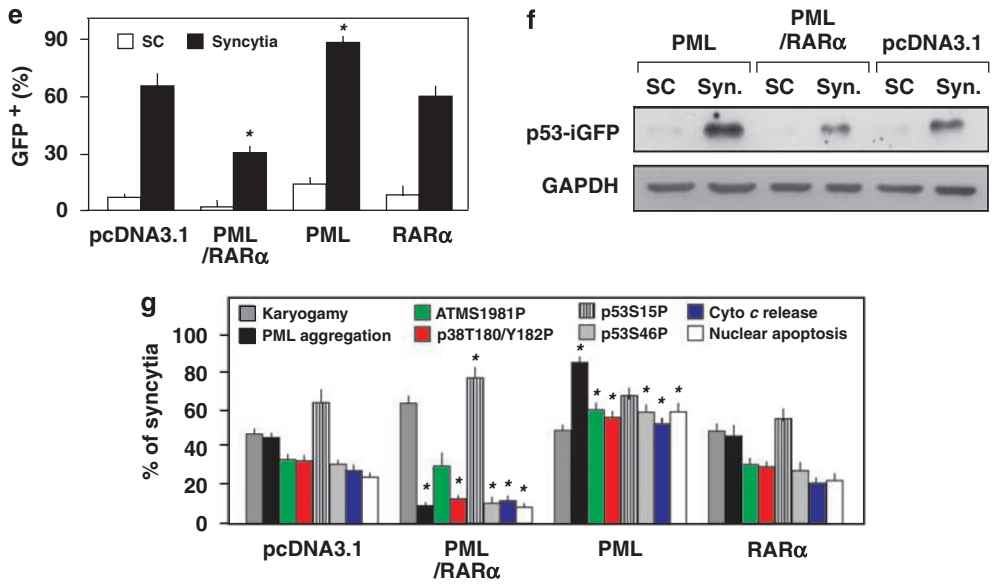

Figure 3 Continued

fusion, AMD3100, yet could be restored by enforcing cell fusion with polyethyleneglycol (PEG), even in the absence of an Env/CD4 interaction (Figure 2a). Thus, chemically induced cell fusion induces similar effects on PML as virally induced fusion, indicating that the phenomenon is not specific for HIV-1-induced syncytia. When karyogamy was inhibited by roscovitin (a chemical inhibitor of Cdk1), transfection with a dominant-negative (DN) mutant of *Cdk1*, rapamycin (a highly selective inhibitor of mTOR), or transfection with the inhibitor of NF-κB super repressor (IKSR), PML aggregation was reduced as well (Figure 2b and c). Inhibition of ATM (with KU-55933 or a small interfering RNA (siRNA) specific for ATM), p38 MAPK (with SB203580, transfection of DN p38, siRNAs specific for p38 or for its activator MAPK kinase (MKK3)), p53 (with cyclic pifithrin-α or DN p53) or caspases (with *N*-benzyloxycarbonyl-Val-Ala-Asp-fluoromethylketone (Z-VAD-fmk) or the baculovirus inhibitor of apoptosis protein p35) all strongly inhibited nuclear chromatin condensation as an internal control of their antiapoptotic activity, yet had no effect on PML aggregation (Figure 2b–d). Altogether, these findings indicate that PML aggregates as a result of cellular and nuclear fusion, upstream of the ATM/p38/p53-dependent apoptotic cascade.

Requirement of PML for the activating phosphorylation of ATM, p38 MAPK and p53. The knockdown of PML with two distinct siRNAs that target all PML isoforms had no effect on the HIV-1 Env-triggered cytoplasmic or nuclear fusion, yet reduced the expression of the p53-inducible protein Bax (Figure 3a). Endogenous PML only marginally colocalized with p53S15P, p53S46P or the p53-phosphorylating kinase p38 in Env-elicited syncytia (Supplementary Figure 2A–C), suggesting that PML must regulate p53 activation in an indirect fashion. Accordingly, PML knockdown inhibited a host of activating phosphorylations (ATM on serine 1981 (ATMS1981P), H2AX (γ-H2AX), p38 MAPK on threonine 180 and tyrosine 182 (p38T180/Y182P) and p53 on serine 46 (S46P)), suggesting that PML acts upstream of the ATM-dependent DNA damage response that triggers syncytial apoptosis.[16] PML knockdown indeed reduced the expression of ATM but not that of H2AX, p38MAPK and p53 (Figure 3a and b). PML depletion had no effect on the karyogamy-associated phosphorylation of p53 on serine 15 (p53S15P) (Figure 3a and b), yet suppressed hallmarks of apoptosis such as mitochondrial Cyt *c* release, caspase-3 activation and nuclear chromatin condensation (Figure 3b).

Similar results were obtained when PML was inhibited by another strategy, by transfection with the oncogenic fusion construct between PML and retinoic acid receptor-α (*PML/RAR*α), which functions as a DN inhibitor of PML.[26,27] Syncytia that were generated from cells transfected with *PML/RAR*α exhibited reduced nuclear PML aggregation and reduced activation of a p53-inducible green fluorescent protein (GFP) reporter gene (Figure 3c–f). Moreover, PML/RARα abolished the entire phosphorylation cascade affecting ATM, p38 MAPK and p53 on serine 46 (but not on serine 15) as well as the hallmarks of syncytial apoptosis (Figure 3g). These data indicate that PML is required for the activation of ATM and the MAP kinase cascade culminating in the phosphorylation of p53 on S46 and apoptosis. In contrast, PML is not required for karyogamy and the mTOR-mediated phosphorylation of p53 on S15.

Physical and/or functional interaction between PML, TopBP1 and ATM. PML inhibition by RNA interference (Figure 3a and b) or *PML-RAR*α (Figure 3g) prevented ATM phosphorylation in HIV-1 Env-elicited syncytia. The contribution of PML to ATM activation was not specific for syncytia, but was also found in normal HeLa cells treated with hydroxyurea (HU), etoposide, ultraviolet C light or γ-irradiation. In all instances, we found that a fraction of phosphorylated ATM (ATMS1981P) colocalized with PML and that the siRNA-mediated knockdown of PML reduced the activating phosphorylation of ATM (Supplementary Figure 3A–D).

These data unraveled a hitherto unsuspected link between PML and ATM in the DNA damage response. We therefore decided to investigate this link in some detail. Extraction of soluble proteins from syncytial nuclei followed by immunofluorescence staining of matrix-linked proteins suppressed the diffuse ATMS1981P staining and revealed puncta of ATMS1981P. This extraction protocol revealed a partial colocalization of PML with γ-H2AX (Supplementary Figure 4A) or with the activated kinase responsible for H2AX phosphorylation, ATMS1981P (Supplementary Figure 4B). Immunoblot experiments revealed that Env-elicited syncytia upregulated several proteins involved in the DNA damage response, in particular topoisomerase IIβ-binding protein-1 (TopBP1) and Rad50 (Figure 4a). TopBP1 and Rad50

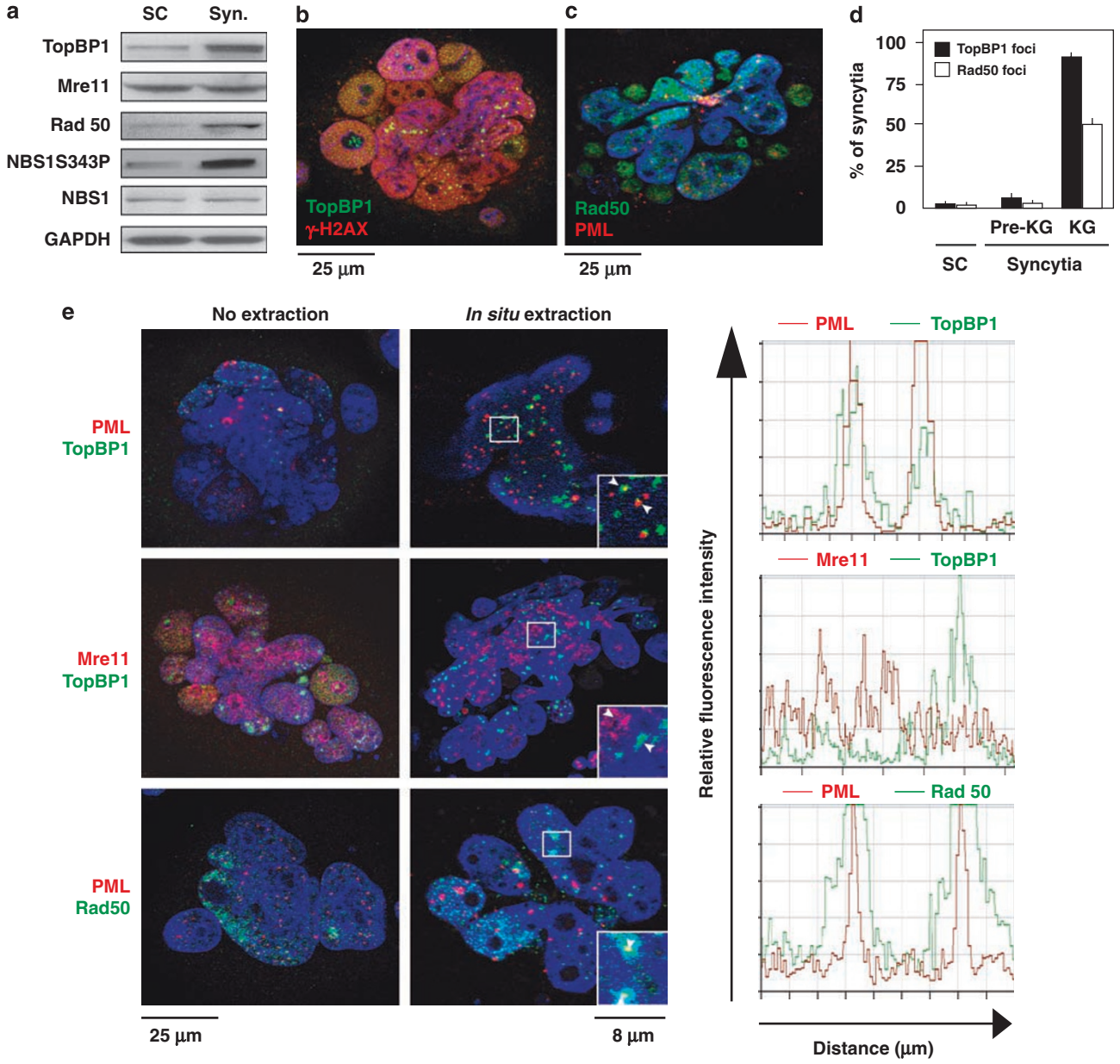

Figure 4 Interaction between PML, TopBP1 and ATM in karyogamic syncytia. (**a**) Increase of TopBP1 expression and NBS1 phosphorylation levels in syncytia. After 36 h of coculture, single cells and karyogamic syncytia were subjected to immunoblot analyses of TopBP1, Mre11, Rad50, NBS1S343P and NBS1. (**b** and **c**) Immunodetection of TopBP1 (**b**) and Rad50 foci (**c**) in karyogamic syncytia. Nuclear localization of TopBP1, Rad50, γ-H2AX and PML was assessed by dual-color immunostaining. (**d**) Quantification of TopBP1 and Rad50 foci in distinct categories of syncytia. Error bars indicate standard deviations of seven independent experiments. (**e**) Partial colocalization of PML with TopBP1 and Rad50 foci. Note the colocalization of extraction-resistant fraction of PML with TopBP1 and Rad50 and the absence of colocalization with Mre11. (**f**) Coimmunoprecipitations of PML and TopBP1. Mixtures of HeLa Env and HeLa CD4 single cells (SC) or syncytia (Syn.) obtained after 24 and 48 h of coculture were lysed and subjected to immunoprecipitation with anti-PML and anti-TopBP1 antibodies. After gel electrophoresis of coimmunoprecipitates, PML and TopBP1 were immunodetected. (**g**) Association between TopBP1 and ATM after 48 h of coculture. Total cell lysates obtained from syncytia (48 h of coculture) (Syn.) or from mixtures of HeLa Env and HeLa CD4 SC were used for immunoprecipitation with anti-TopBP1 and anti-ATM antibodies. Western blotting was performed with anti-TopBP1 antibody

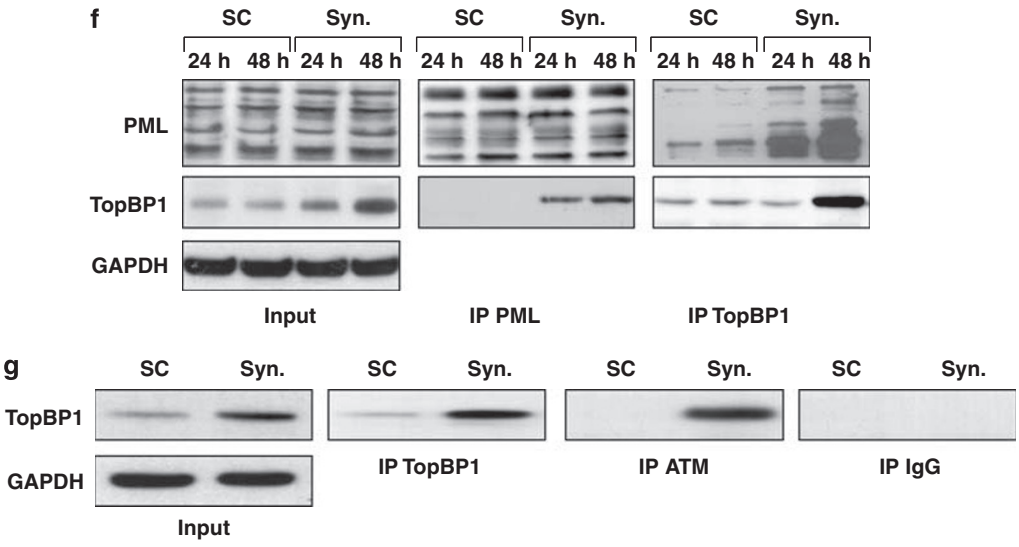

Figure 4 Continued

accumulated in syncytial nuclei, in discrete foci (Figure 4b–d). TopBP1 and Rad50 colocalized in part with PML after *in situ* extraction (Figure 4e), and TopBP1 immunoprecipitated with PML and ATM, more so in syncytia than in SCs (Figure 4f and g).

As PML can regulate the stability of TopBP1,[23] we investigated the contribution of TopBP1 to the apoptotic cascade triggered by HIV-1 Env. Knockdown of PML reduced the syncytial expression of TopBP1, Nijmegen breakage syndrome 1 (NBS1) (Figure 5a) and ATM (Figure 3a). Knockdown of TopBP1 with two distinct siRNAs (Supplementary Figure 5A) had no effect on the abundance of PML, yet reduced the amount of NBS1 and ATM in syncytia (Figure 5b). TopBP1 depletion shifted the diffuse phosphorylation of ATM to discrete foci, reduced the size of PML nuclear bodies in syncytia (Figure 5c) and reduced the amount of PML that coimmunoprecipitated with ATM (Supplementary Figure 5B), proportional to the overall reduction of ATM protein (Figure 5b and Supplementary Figure 5B). TopBP1 depletion strongly inhibited ATM phosphorylation, MAPK activation, p53S46P and apoptosis (Figure 5d and e). NBS1 depletion (Supplementary Figure 5C) reduced the size of PML bodies (Figure 5c), had no effect on the recruitment of TopBP1 into discrete nuclear foci (Figure 5d), yet suppressed ATM phosphorylation (Figure 5c and d) and all downstream events (Figure 5e). In contrast with NBS1 depletion, ATM depletion had no effect on the size of PML that remained as large as in untreated syncytia (mostly $>0.5\,\mu$m) (Figure 5c). Depletion of PML, TopBP1, NBS1 and ATM all inhibited apoptosis at a similar level of efficacy and prevented the phosphorylation of ATM substrates such as H2AX with a similar potency (Figure 5d and e).

These results indicate the existence of a molecular aggregate including PML, TopBP1, NBS1 and ATM that engages in a complex regulatory circuitry. PML controls the overall expression level of the three other proteins (TopBP1, NBS1 and ATM) as well as the aggregation of TopBP1 and ATM in discrete foci. TopBP1, in turn, controls the abundance of NBS1 and ATM (and exerts a mild effect on the size of PML bodies), whereas NBS1 had no effect on the abundance of the other proteins, controls the size of PML bodies and is required for the phosphorylation of ATM.

HIV-induced PML aggregation *in vivo*. HIV-1-induced syncytia, the so-called 'multinuclear giant cells', are most easily detectable in histological sections of the frontal cortex, where they constitute the principal diagnostic marker of HAE.[14,28] The nuclei of such HAE-associated syncytia exhibited PML aggregation whereas normal neurons or glial cells did not, as determined by immunohistochemistry (Figure 6a). The frequency of brain syncytia with aggregated PML was higher than that of syncytia that stained positively after terminal deoxyuridine nucleotide end labeling staining (which detects DNA fragmentation), in accord with the idea that PML aggregation occurs before apoptosis (Figure 6a). Similar results were obtained when we analyzed bona fide syncytia present in lymph nodes from

Figure 5 PML-dependent expression of TopBP1 and NBS1 controls the syncytial activation of ATM. HeLa CD4 and HeLa Env cells were individually transfected with the indicated siRNAs and cocultured (or not) for 48 h. Then, cell lysates were prepared and western blot analysis (**a** and **b**) or immunofluorescence staining (**c**–**e**) was performed. (**a**) Effect of PML knockdown on TopBP1 and NBS1 expression. Total protein lysates were subjected to western blot analysis for PML, TopBP1, NBS1S343P, NBS1 and Mre11. Note that the knockdown of PML provoked the decrease of TopBP1 and NBS1 expression in syncytia. (**b** and **c**) Effect of TopBP1 downmodulation by RNA interference on ATM activation. Note that TopBP1 depletion reduced NBS1 and ATM expression (**b**). A partial reduction in the size of PML nuclear bodies and appearance of ATM discrete foci were also observed (**c**). Note that PML expression was not affected (**b**). (**d** and **e**) Effects of TopBP1 or NBS1 inhibition on the pro-apoptotic pathway elicited by Env. After 48 h of coculture, transfected cells were fixed, permeabilized and stained for immunofluorescence analysis (as performed in Figures 2 and 3). Error bars indicate standard deviations of six independent experiments. Asterisks indicate significant ($P<0.001$) effects

untreated HIV-1 carriers. Such syncytia, as well as a fraction of mononuclear cells, exhibited an enhanced nuclear staining for PML (Figure 6b). Moreover, a fraction of peripheral blood mononuclear cells (PBMCs) from untreated HIV-1$^+$ donors contained aggregated PML and overexpressed TopBP1, correlating with viral load (Figure 6c). The frequency of

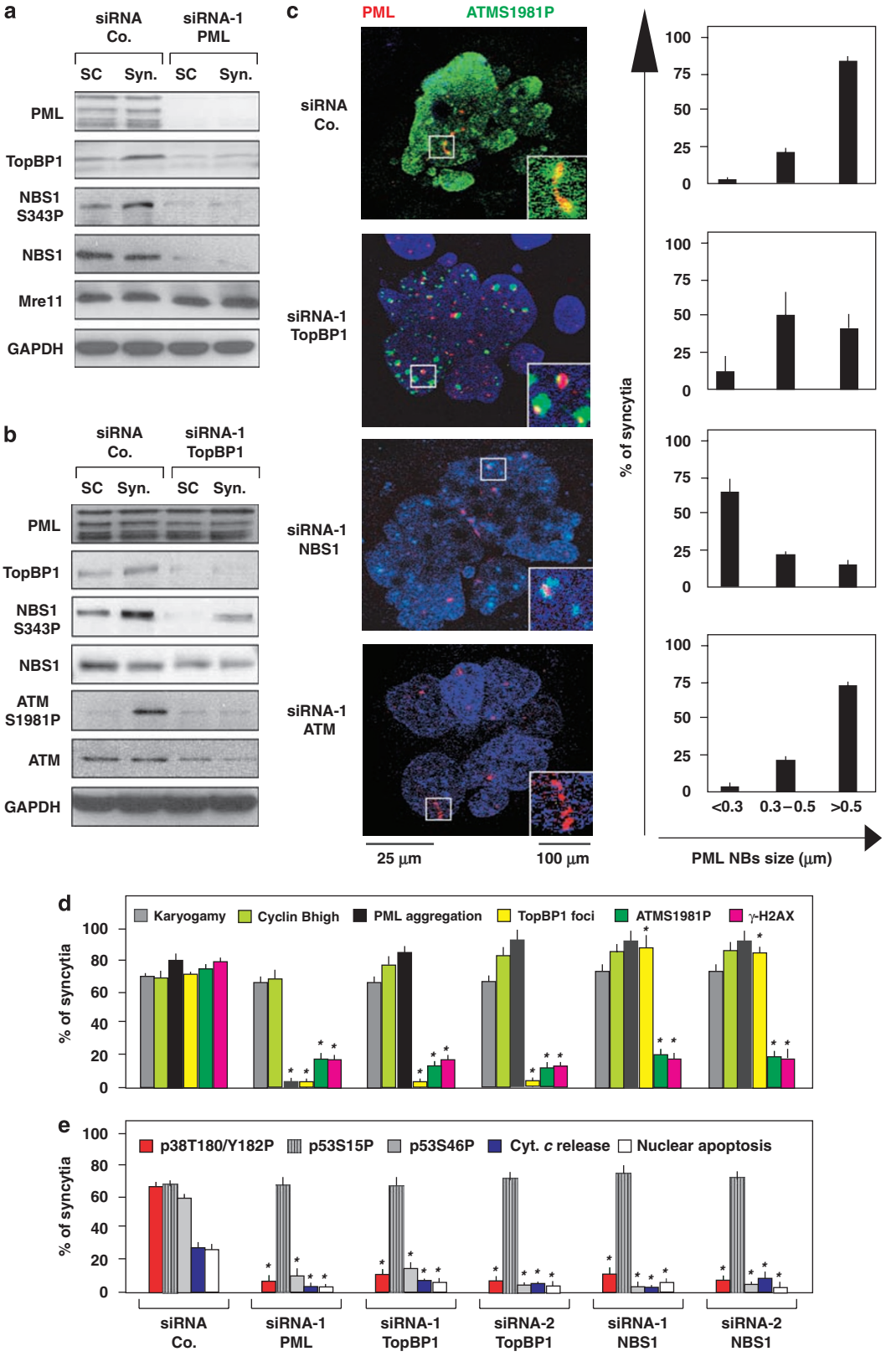

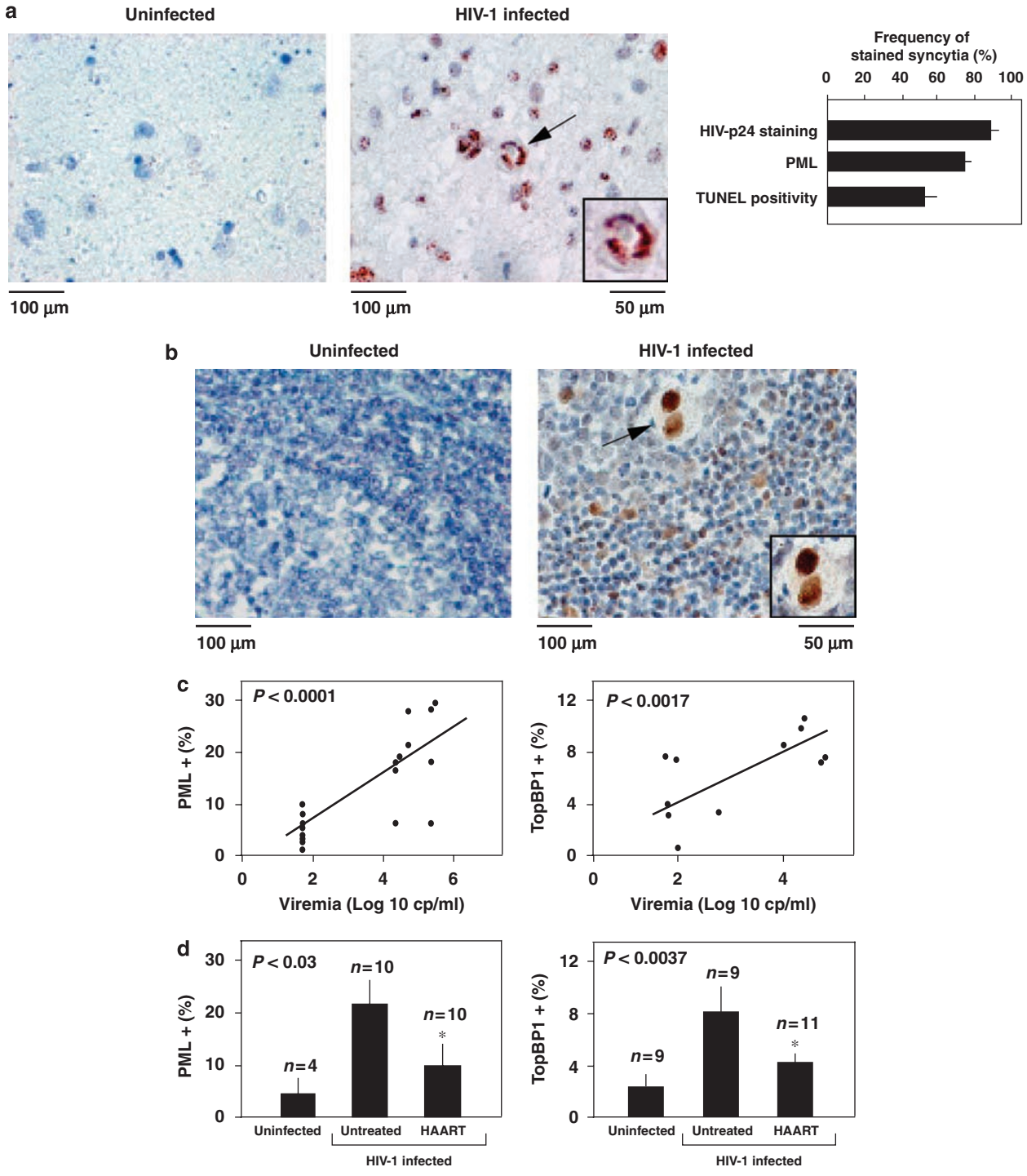

Figure 6 PML aggregation *in vivo*, in HIV-1-infected patients. (**a**) PML aggregation in syncytia detectable in frontal cortex from patients with HIV-1-associated encephalitis (HAE). PML were visualized by immunohistochemistry on histological sections from control patients or from untreated HIV-1 carriers with HAE but without opportunistic infection. Arrows indicate giant multinuclear cells. The percentage of syncytia ($X \pm$ S.E.M.) staining positively for PML amounted to 73 ± 7, as determined for six different HIV-1 carriers, whereas $<5\%$ of mononuclear cells were positive. (**b**) PML aggregation in lymph nodes from controls and untreated HIV-1 carriers. Arrows mark bona fide syncytia. (**c** and **d**) Correlation between PML aggregation, TopBP1 overexpression, viral status and HAART treatment. PBMCs from untreated patients were subjected to PML and TopBP1 staining and the values were plotted against the number of viral particles in the serum. *P*-values refer to the correlation coefficients (**c**). Moreover, a cohort of HIV-1$^-$ donors, untreated HIV-1 carriers and HAART-treated subjects with undetectable viremia were analyzed for PML aggregation (**d**)

PBMC with aggregated PML or overexpressed TopBP1 was reduced in a cohort of patients treated by highly active antiretroviral therapy (Figure 6d). These results demonstrate that the activation of PML does occur *in vivo*, in the central nervous, as well as in the lymphoid, system of patients infected with HIV-1.

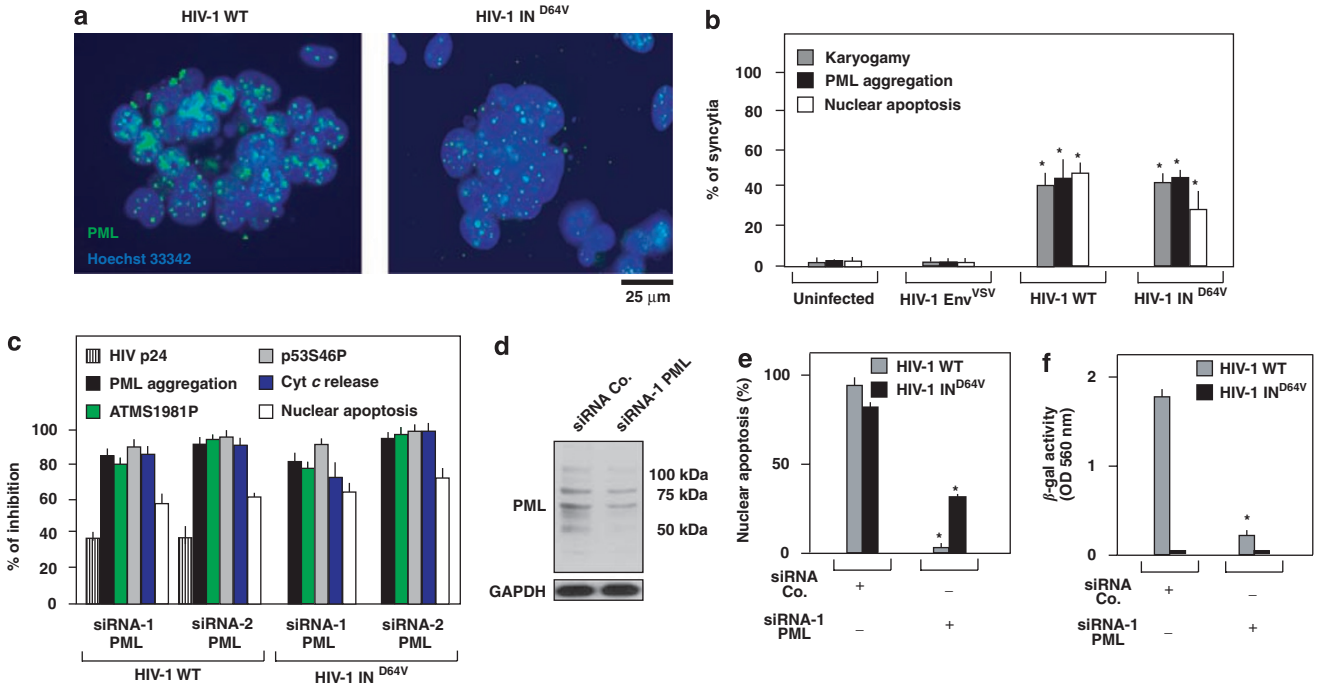

Figure 7 Involvement of PML in syncytial apoptosis of HIV-1-infected CD4$^+$ cell lines. (**a**–**c**) CD4$^+$ HeLa cells were infected with HIV-1 WT, HIV-1 Env^{VSV} or HIV1 IN^{D64V} at an MOI of 10 for 36 h and then stained for PML (**a**). The percentage ($X \pm$ S.D., $n = 3$) of syncytia that exhibited PML aggregation was measured (**b**). CD4$^+$ HeLa cells were transfected with a control siRNA or specific siRNAs depleting PML. Thirty-six hours later, cells were infected with HIV-1 WT or HIV1 IN^{D64V} at an MOI of 10 for 48 h, and the expression of the viral protein p24, the aggregation of PML, the phosphorylation of ATM or p53, and apoptosis were quantified (**c**). Results are plotted as the percent inhibition of the indicated parameters determined for syncytia. (**d**–**f**) Effect of PML knockdown on the syncytial apoptosis of HIV-1-infected CEM T cells. CEM cells were infected with a retrovirus vector expressing a control siRNA or an siRNA specific for PML and the depletion of PML was controlled by immunoblotting (**d**). Cells were then infected with wild-type HIV-1 and nuclear apoptosis was determined 72 h later (**e**). Moreover, the number of infectious viruses contained in the culture supernatant was determined (**g**). Results are means ± S.D. of four independent experiments. Asterisks indicate significant ($P < 0.001$) effects

Requirement of PML for apoptosis induction by HIV-1. Within 48 h after infection of CD4$^+$CXCR4$^+$ HeLa cells with the syncytium-inducing wild-type (WT) HIV-1^{LAI} strain, a significant fraction of cells, preferentially syncytia, underwent apoptosis. A similar degree of syncytial apoptosis was observed when cells were infected with an HIV-1 mutant lacking integrase activity due to a point mutation (HIV-1 IN^{D64V}) that was otherwise identical to the WT HIV-1^{LAI} strain (Figure 7a and b). A much less syncytium formation and apoptosis was detected when the endogenous HIV-1 *env* gene was replaced by that of vesicular stomatitis virus (VSV) (HIV-1 Env^{VSV}), which is not fusogenic (not shown, Lum *et al*.[29]). Importantly, infection with HIV-1 IN^{D64V} (but not HIV-1 Env^{VSV}, not shown) was as efficient in eliciting PML aggregation as was infection with HIV-1 WT (Figure 7a and b).

The siRNA-mediated depletion of PML markedly inhibited (by $>70\%$) apoptosis induction by HIV-1 WT or HIV-1 IN^{D64V} in HeLa CD4$^+$ cells (Figure 7b, Supplementary Figure 6A and B). In addition, PML knockdown partially reduced (by 30–40%) the expression of p24 by HIV-1^{LAI}-infected cells (Figure 7c), thus confirming an earlier study showing that PML can influence viral replication.[30] In syncytia induced by either HIV-1 WT or HIV-1 IN^{D64V}, PML knockdown also inhibited (by $>60\%$) the activating phosphorylations of ATM, p38 MAPK and p53S46P and consequent apoptosis (Figure 7c). To confirm these results in another cellular context, we generated CEM T cells that stably reduced PML expression after infection with a retrovirus encoding a PML-specific shRNA. This technique of PML depletion (Figure 7d) also reduced the HIV-1 WT- or HIV-1 IN^{D64V}-induced cytopathic effect (Figure 7e) and decreased the replication of HIV WT (Figure 7f).

Primary human PHA blasts infected with HIV-1 *in vitro* manifested PML aggregation within syncytia (Figure 8a). This result was obtained after infection with either HIV-1 WT or HIV-1 IN^{D64V}, indicating that retroviral integration into the host genome (which depends on the HIV-1 integrase) is not required for PML aggregation. Knockdown of PML with a lentiviral shRNA construct (Figure 8b) reduced the phosphorylation of ATM (Figure 8c) and its substrate γ-H2AX (Figure 8d) in syncytia elicited by HIV-1 WT or HIV-1 IN^{D64V} among such primary T cells. Concomitantly, PML depletion reduced nuclear apoptosis (Figure 8e) and HIV-1 replication (Figure 8f). These results underscore the critical role of PML in syncytial apoptosis of primary T lymphocytes infected by HIV-1.

Discussion

Host gene products play a major role in the (loss of) control of viral replication and viral cytopathicity. On theoretical grounds,

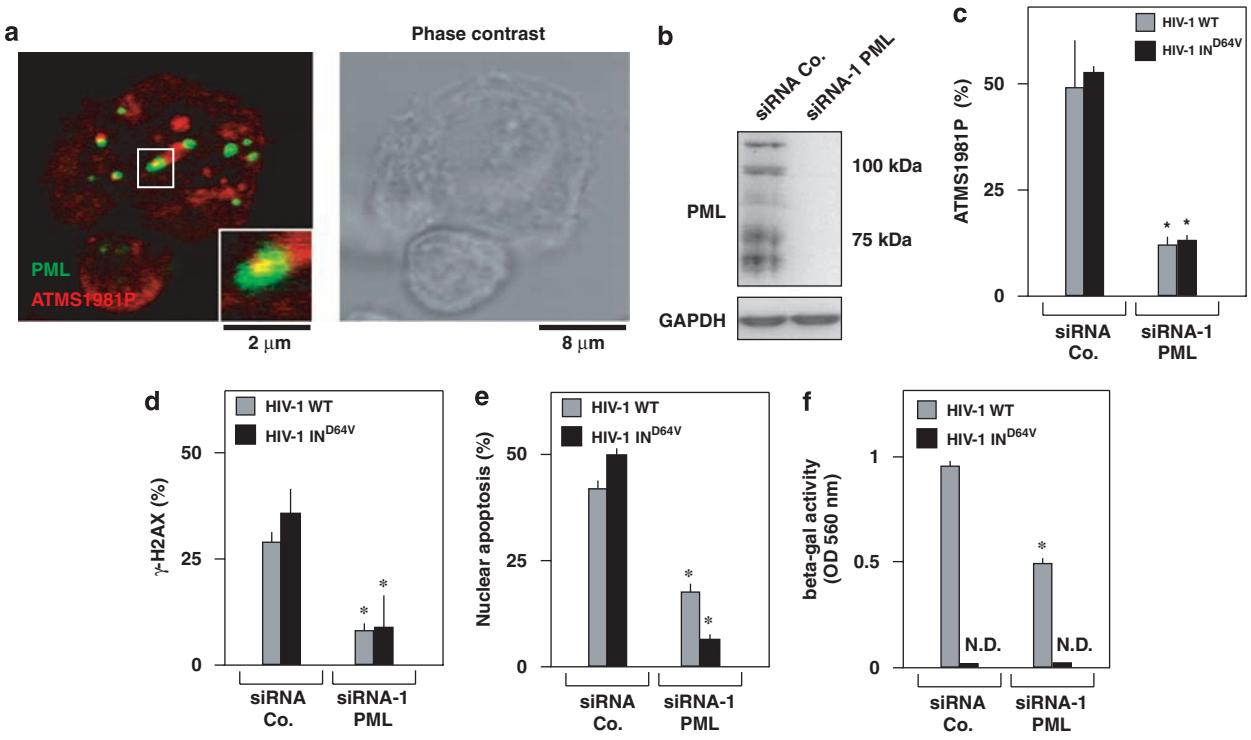

Figure 8 Involvement of PML in syncytial apoptosis of HIV-1-infected primary human lymphoblasts. PHA/IL-2 lymphoblasts obtained from healthy donors were infected with HIV-1 WT and HIV1 IN^{D64V} at an MOI of 10 for 48 h and then stained for the indicated markers. (**a**) Partial colocalization of PML and ATMS1981P in syncytia was identified by immunofluorescence after infection of PHA/IL-2 lymphoblasts with HIV-1 WT. (**b**–**f**) Effects of PML depletion. PHA/IL-2 lymphoblasts that were transduced with a lentivirus containing a PML-specific siRNA or a control vector (**b**) were infected with HIV-1 WT or HIV1 IN^{D64V} at an MOI of 10 for 48 h (as in figure). The phosphorylation status of ATM (**c**), H2AX (**d**) and apoptosis were quantified (**e**). The effect of PML depletion on HIV-1 infection was evaluated by measuring β-galactosidase activity (as described in Materials and Methods) (**f**). Asterisks indicate significant ($P<0.001$) effects

antiviral strategies that target host proteins rather than viral gene products would have the advantage of a reduced probability of viral escape (because host proteins rarely mutate). Here, we demonstrate that syncytium formation induced by Env (in an HIV-1-free system, Figures 1–5) or HIV-1 infection (Figures 6–8) triggers an apoptotic pathway that involves the action of PML (Supplementary Figure 7). An earlier report suggested that PML is recruited to recently formed HIV pre-integration complexes and ameliorates HIV-1-mediated transduction.[30] Our present study unravels a novel completely distinct role for PML in HIV-1 infection, in a pro-apoptotic signal transduction pathway that is independent of HIV-1 integrase, but dependent on the fusogenic action of Env.

In Env-elicited syncytia, PML aggregation is an early event that is triggered by karyogamy (Figure 1). At present, it is not known what exact molecular events account for this karyogamy-dependent PML aggregation, although, in analogy to other system,[22] PML might sense some kind of cellular stress elicited by the formation of syncytia. The PML bodies from normal cells and those from syncytia shared some characteristics (colocalization with SUMO-1 and DAXX but not with nucleolin and MDM2), yet differed in others, in particular in the size of the PML bodies (that increased in syncytia) (Figure 5c, Supplementary Table 1), in accord with their dynamic nature.[22,31] In addition, PML bodies from SCs and syncytia differed in their colocalization/coimmunoprecipitation with elements of the DNA damage response including ATM, γ-H2AX, TopBP1 and RAD50 (Figures 1, 4 and 5, Supplementary Figure 4, Supplementary Table 1). There was clearly an increase in the interaction between these latter proteins and PML in syncytia, suggesting that the 'aggregated' PML bodies (in syncytia), as opposed to 'normal' PML bodies (in SCs), sense DNA damage triggered by the fusion of non-synchronized nuclei.

It should be noted that PML aggregation was induced by different kinds of physical or chemical DNA damage, even in SCs (Supplementary Figure 3). Moreover, we found that a particular type of PML aggregation could be induced by mitotic catastrophe. Mitotic catastrophe can be induced in syncytia by inhibiting the checkpoint kinase-2 (Chk2). Although untreated syncytia arrest their cell cycle in G2, Chk2-inhibited syncytia enter a multipolar catastrophic mitosis, followed by accelerated apoptosis.[32] In these conditions, we found that syncytia with aberrant mitotic figures manifested a major aggregation of PML in spots that were even larger than those found in karyogamic nuclei, yet were not associated with chromatin (Supplementary Figure 8A). As knockdown of PML inhibited signs of apoptosis (such as Cyt *c* release and nuclear apoptosis) and did not impede the appearance of multipolar aberrant mitoses (Supplementary Figure 8B and C), we

conclude that PML is also involved in sensing DNA stress in the context of mitotic catastrophe. Altogether, these results suggest that PML has a general role in 'sensing' DNA damage or 'genomic stress'.

In karyogamic syncytia, PML aggregation occurs upstream of ATM phosphorylation (and not vice versa) because PML depletion impeded ATM phosphorylation, whereas depletion or inhibition of ATM had no effects on PML aggregation. Our results indicate that PML and ATM colocalize and/or coimmunoprecipitate in a molecular complex that includes other proteins involved in the DNA damage response including TopBP1 and NBS1. PML depletion reduced the abundance of TopBP1, NBS1 and ATM, whereas TopBP1 depletion only reduced NBS1 and ATM (but not PML). Depletion of either TopBP1 or NBS1 reduced the size of PML bodies, whereas ATM depletion had no such effect. Knockdown of PML, TopBP1 and NBS1 all had a similar inhibitory effect on ATM phosphorylation, the phosphorylation of ATM substrates and downstream events leading to apoptosis (Figure 5). These results suggest that PML, TopBP1, NBS1 and ATM interact within a syncytium-associated nuclear complex in which ToBP1 and NBS1 act as functional links between PML and ATM. However, in view of the complex regulation of DNA damage foci,[33] it is difficult to establish a linear hierarchy among these factors.

There are multiple mechanisms through which PML can modulate the activity of p53, which is the most important pro-apoptotic transcription factor in syncytia.[9] As a possibility, PML may inactivate the principal negative regulator of p53, MDM2, by sequestering it to the nucleolus.[34] However, in HIV-1 Env-elicited syncytia, MDM2 and PML do not colocalize (Supplementary Figure 2C), and MDM2 remains largely cytoplasmic.[6] It has also been suggested that PML would stimulate the phosphorylation of p53 on serine 46 by homeodomain-interacting protein kinase 2 (HIPK2).[35] However, the knockdown of HIPK2 did not influence p53S46 phosphorylation in this system.[8] Finally, it has been suggested that PML nuclear bodies would recruit p53 to enhance p53 transactivation.[36,37] However, in HIV-1 Env-elicited syncytia, PML and active phosphorylated p53 did not colocalize in karyogamic syncytia (Supplementary Figure 2A and B). Rather, our data indicate that PML influences p53 phosphorylation indirectly, through ATM and p38 MAPK. Both ATM and p38 MAPK are required for the phosphorylation of p53 in syncytia, and PML depletion inhibits the activation of ATM and p38MAPK (Figure 3).

It should be noted that all the elements of the pathway delineated thus far (PML→ATM→p38MAPK→p53) have been detected *in vivo*, in multinuclear giant cells of the HAE brain, lymph node biopsies, as well as a sub-population of PBMC (see Figure 6 as well as Perfettini *et al*.[8,9,16]; Castedo *et al*.[15]; and Nardacci *et al*.[17]). This implies that the results obtained *in vitro*, in the Env-elicited syncytia, can be extrapolated – with the necessary caution – to the pathogenesis of AIDS. Furthermore, single-nucleotide polymorphisms in the PML gene correlate with HIV disease progression *in vivo*.[38] The data presented here provide the first rationale to explain how mutations that affect the expression or structure of PML might impact on AIDS pathogenesis.

Materials and Methods

Antibodies, plasmids and reagents. Monoclonal (PG-M3) and polyclonal (H-238) antibodies for the detection of PML were obtained from Santa-Cruz Biotechnology Inc. Polyclonal rabbit antibodies for the detection of MKK3, MKK3 with phosphorylated serine 189 and/or MKK6 with phosphorylated serine 207, p38, p38T180/Y182P, p53S15P, p53S46P and SUMO-1 were from Cell Signaling Technology. Monoclonal antibodies against cyclin B1 or anti-Cyt *c* were purchased from Becton Dickinson. The polyclonal rabbit antibody against NBS1 was obtained from Calbiochem. The monoclonal antibody against NBS1S343P was from Interchim. Monoclonal antibodies used to reveal ATM, ATMS1981P, H2AX H2AXS139P, hMRE11 and Rad50 were obtained from Upstate and anti-GFP antibody, Hoechst 33342 and TOPRO3 were purchased from Invitrogen. The plasmid for Baculovirus p35 was provided by Dr. Guy Salvesen (Burnham Institute, La Jolla, CA, USA). DN mutant plasmids for Cdk1 (DN Cdk1), IKSR, DN p53 (H175) and DN p38 MAPK were described earlier.[9] The WT X4 HIV-1 proviral clone pNL4-3 and the VSV G protein (VSV-G)-pseudotyped HIV-1-based vector system have been described earlier.[39] WT X-4 HIV-1 proviral clone pNL4-3 containing the inactivating integrase mutation Q62A (HIV-1 IN$^-$) was a gift from C Petit and P Sonigo (Institut Pasteur, Paris, France) and the WT X-4 HIV-1 proviral clone pNL4-3 deleted in envelope gene (HIV-1 ENV-) was a gift from O Schwartz (Institut Pasteur). Where indicated, cells were treated with roscovitin and SB203580 (Calbiochem-Novabiochem), AMD3100, rapamycin, HU, VP16 and PEG (all from Sigma-Aldrich), pifithrin-α, Z-VAD-fmk (all from Bachem) and Chk2 inhibitor II (Calbiochem). KU-55933 was obtained from Dr. Mark O'Connor and Graeme Smith (Kudos, Cambridge, UK).

Cell lines, cell culture and transfection. HeLa cells stably transfected with the *Env* gene of HIV-1 LAI/IIIB (HeLa Env) and HeLa cells transfected with *CD4* (HeLa CD4) were cultured alone or together at a ratio of 1 : 1 in Dulbecco's modified Eagle's medium supplemented with 10% FCS, 2 mM L-glutamine and penicillin/streptomycin (Invitrogen) in the absence or in the presence of 1 μM roscovitin, 1 μM rapamycin, 100 nM SB203580, 10 μM cyclic pifithrin-α or 100 μM Z-VAD-fmk during indicated times. Transfections of plasmids were performed with lipofectamine 2000 (Invitrogen) 24 h before cell fusion. Human lymphoid cell line CEM4fx was grown in RPMI medium (Gibco).

Immunoblots and immunoprecipitation. Total cellular proteins were extracted in 250 mM NaCl-containing lysis buffer (250 mM NaCl, 0.1% NP40, 5 mM EDTA, 10 mM Na_3VO_4, 10 mM NaF, 5 mM DTT, 3 mM $Na_4P_2O_7$ and protease inhibitor cocktail). Protein extracts (50 μg) were run on 3 or 12% SDS-PAGE and transferred at 4°C onto a nitrocellulose membrane. After incubation for 12 h in the blocking buffer (Zymed), the membranes were incubated with indicated primary antibodies at room temperature during 1 h 30 min. Then, horse radish peroxidase-conjugated goat anti-rabbit or goat anti-mouse (Southern Biotechnology) antibodies were incubated during 1 h and revealed with the enhanced ECL detection system. For immunoprecipitation, lysates (200 μg) were immunoprecipitated with anti-ATM, anti-PML or anti-TopBP1 antibodies for 2 h and incubated overnight at 4°C with G-coupled sepharose beads (Roche Applied Science, Rockford, IL, USA), washed five times with lysis buffer and subjected to SDS-PAGE.

Immunofluorescence and immunohistochemistry. Cocultures were fixed in 4% paraformaldehyde/phosphate-buffered saline (PBS) for 30 min, permeabilized in 0.1% SDS in PBS and incubated with FCS for 20 min. Then, indicated sera were used for immunodetection in PBS containing 1 mg/ml BSA and revealed with goat anti-rabbit IgG conjugated to Alexa 488 (green) or Alexa 568 (red) fluorochrome from Invitrogen. To assess karyogamy and nuclear apoptosis, cells were counterstained with Hoechst 33342 (Invitrogen). Proteins attached to damaged nuclear matrix were detected by immunofluorescence microscopy using the following procedure. Briefly, living cells were incubated for 20, 10 and 5 min with a fractionation buffer (containing 50 mM Hepes, 150 mM NaCl, 1 mM EDTA, 0.2% NP40, 10 mM NaF, 10 mM glycerophosphate, 1 mM Na_3VO_4 and protease inhibitor cocktail) at 4°C before fixation. Immunohistochemistry was performed following published protocols.[8,9,17]

RNA interference. Published siRNAs specific for ATM,[40] NBS1 (hNBS1.1 CAGGAGGAAGATGTCAATGdTdT or hNBS1.2 GGCGUGUCAGUUGAUGAAA dTdT), MKK3 (hMEKK3 GCACGGUCGACUGUUUCUAdTdT), PML (PML1.1 from Santa-Cruz or PML1.2: hPML-1225 CUCCCAGGGACCCUAUUGAdTdT), p38MAPK (Dharmacon RNATtechnology) and TopBP1 (hTopBP1.1 CUCACCUUA UUGCAGGAGAdTdT or TopBP1.2 GAACGUGGUGGCUCUAAAUdTdT) were

transfected using Oligofectamine (Invitrogen), according to the manufacturer's instructions. For stable expression of short interfering RNAs against PML into CEM cell lines, the retroviral GeneSuppressor kit (Imgenex) was used. The retroviral siRNA plasmid (IMG-1000-1) included in the kit has been modified from pCLNCX vector. It contains the neomycin-resistance gene (G418) under the control of 5′-LTR and a cloning site downstream of the U6 promoter for the expression of hairpin siRNA. Double-stranded oligonucleotide targeting PML gene was synthesized and introduced into the IMG-1000-1 plasmid (linearized pSuppressor retro; Imgenex). This plasmid was referred to as pSupPML. We used the IMG-1000-6 plasmid Imgemex (that codes for a scrambled siRNA) as a negative control (pSup). The plasmids pSupPML and pSup were independently cotransfected with the plasmid pCL-Ampho (Amphotropic RetroMax packaging vector; Imgenex) into 293T cells using the calcium phosphate procedure. Titers of produced retroviral vectors (SupPML and pSup) were determined after infection of HeLa cells and G418 selection. CEM4fx cells were infected at a multiplicity of infection of 1. Twenty-four hours later, infected cells were selected with G418 (1 mg/ml) and amplified as a polyclonal population of cells stably transduced with pSup (CEM-control) or pSupPML (CEM-PML$^-$).

Viral and pseudoviral constructs. Viral stocks of WT X4 HIV-1, VSV-G-pseudotyped HIV-1 and X4 HIV-1 containing integrase mutation Q62A were obtained after transfection of 293T with virus-encoding plasmids as described earlier.[16]

Patients. Axillary lymph node biopsies were obtained from healthy and HIV-1-infected individuals (all men, mean age 36 years, with a plasma viral load >105 copies/ml). Plasma HIV-1 RNA levels were determined by the bDNA procedure (Versant HIV RNA 3.0; Bayer, USA). Post-mortem frontal cortex sections were obtained from seven brains of patients with HIV-1-associated dementia (but lacking secondary infections) and four control brains obtained from uninfected control patient. Human samples were obtained with written informed consent in accord with the National and European legal requirements, after approval by the Institutional Review Board of the National Institute for Infectious Disease and the Medical Faculty of the University of Rome.

Acknowledgements. We declare no conflicting financial interests. We thank the NIH AIDS Research and Reference Reagent Program (Bethesda, MD) for reagents, KuDOS Pharmaceuticals (Cambridge, UK) for providing KU-55933, Nathanaël Larochette and Didier Métivier (INSERM U848, Villejuif, France) for technical help. We thank Nazanine Modjtahedi (INSERM U848, Villejuif, France) for helpful advice. This study has been supported by a special grant from LNC, as well as grants by ANRS, Sidaction and the European Commission (RIGHT, ACTIVE P53, ApoSys) (to GK), Istituto Superiore di Sanità (no. 40F60, Ricerca Corrente e Finalizzate 'Ministerio della Saluté', COFIN from MIUR and AIRC).

1. Galluzzi L, Brenner C, Morselli E, Touat Z, Kroemer G. Viral control of mitochondrial apoptosis. *PLoS Pathog* 2008; **4**: e1000018.
2. Cossarizza A. Apoptosis and HIV infection: about molecules and genes. *Curr Pharm Des* 2008; **14**: 237–244.
3. Gougeon ML. Apoptosis as an HIV strategy to escape immune attack. *Nat Rev Immunol* 2003; **3**: 392–404.
4. Perfettini JL, Castedo M, Roumier T, Andreau K, Nardacci R, Piacentini M *et al.* Mechanisms of apoptosis induction by the HIV-1 envelope. *Cell Death Differ* 2005; **12** (Suppl 1): 916–923.
5. Garg H, Joshi A, Freed EO, Blumenthal R. Site-specific mutations in HIV-1 gp41 reveal a correlation between HIV-1-mediated bystander apoptosis and fusion/hemifusion. *J Biol Chem* 2007; **282**: 16899–16906.
6. Castedo M, Ferri KF, Blanco J, Roumier T, Larochette N, Barretina J *et al.* Human immunodeficiency virus 1 envelope glycoprotein complex-induced apoptosis involves mammalian target of rapamycin/FKBP12-rapamycin-associated protein-mediated p53 phosphorylation. *J Exp Med* 2001; **194**: 1097–1110.
7. Andreau K, Perfettini JL, Castedo M, Metivier D, Scott V, Pierron G *et al.* Contagious apoptosis facilitated by the HIV-1 envelope: fusion-induced cell-to-cell transmission of a lethal signal. *J Cell Sci* 2004; **117**: 5643–5653.
8. Perfettini JL, Castedo M, Nardacci R, Ciccosanti F, Boya P, Roumier T *et al.* Essential role of p53 phosphorylation by p38 MAPK in apoptosis induction by the HIV-1 envelope. *J Exp Med* 2005; **201**: 279–289.
9. Perfettini JL, Roumier T, Castedo M, Larochette N, Boya P, Raynal B *et al.* NF-kappaB and p53 are the dominant apoptosis-inducing transcription factors elicited by the HIV-1 envelope. *J Exp Med* 2004; **199**: 629–640.
10. Ferri KF, Jacotot E, Blanco J, Este JA, Zamzami N, Susin SA *et al.* Apoptosis control in syncytia induced by the HIV type 1-envelope glycoprotein complex: role of mitochondria and caspases. *J Exp Med* 2000; **192**: 1081–1092.
11. Etemad-Moghadam B, Sun Y, Nicholson EK, Fernandes M, Liou K, Gomila R *et al.* Envelope glycoprotein determinants of increased fusogenicity in a pathogenic simian-human immunodeficiency virus (SHIV-KB9) passaged *in vivo*. *J Virol* 2000; **74**: 4433–4440.
12. Camerini D, Su HP, Gamez-Torre G, Johnson ML, Zack JA, Chen IS. Human immunodeficiency virus type 1 pathogenesis in SCID-hu mice correlates with syncytium-inducing phenotype and viral replication. *J Virol* 2000; **74**: 3196–3204.
13. Blaak H, van't Wout AB, Brouwer M, Hooibrink B, Hovenkamp E, Schuitemaker H. *In vivo* HIV-1 infection of CD45RA(+)CD4(+) T cells is established primarily by syncytium-inducing variants and correlates with the rate of CD4(+) T cell decline. *Proc Natl Acad Sci USA* 2000; **97**: 1269–1274.
14. Gonzalez-Scarano F, Martin-Garcia J. The neuropathogenesis of AIDS. *Nat Rev Immunol* 2005; **5**: 69–81.
15. Castedo M, Roumier T, Blanco J, Ferri KF, Barretina J, Tintignac LA *et al.* Sequential involvement of Cdk1, mTOR and p53 in apoptosis induced by the HIV-1 envelope. *EMBO J* 2002; **21**: 4070–4080.
16. Perfettini JL, Nardacci R, Bourouba M, Subra F, Gros L, Seror C *et al.* Critical involvement of the ATM-dependent DNA damage response in the apoptotic demise of HIV-1-elicited syncytia. *PLoS ONE* 2008; **3**: e2458.
17. Nardacci R, Antinori A, Larocca LM, Arena V, Amendola A, Perfettini JL *et al.* Characterization of cell death pathways in human immunodeficiency virus-associated encephalitis. *Am J Pathol* 2005; **167**: 695–704.
18. Bernardi R, Pandolfi PP. Structure, dynamics and functions of promyelocytic leukaemia nuclear bodies. *Nat Rev Mol Cell Biol* 2007; **8**: 1006–1016.
19. Gurrieri C, Capodieci P, Bernardi R, Scaglioni PP, Nafa K, Rush LJ *et al.* Loss of the tumor suppressor PML in human cancers of multiple histologic origins. *J Natl Cancer Inst* 2004; **96**: 269–279.
20. Kogan SC, Hong SH, Shultz DB, Privalsky ML, Bishop JM. Leukemia initiated by PMLRARalpha: the PML domain plays a critical role while retinoic acid-mediated transactivation is dispensable. *Blood* 2000; **95**: 1541–1550.
21. Zhang P, Chin W, Chow LT, Chan AS, Yim AP, Leung SF *et al.* Lack of expression for the suppressor PML in human small cell lung carcinoma. *Int J Cancer* 2000; **85**: 599–605.
22. Dellaire G, Ching RW, Ahmed K, Jalali F, Tse KC, Bristow RG *et al.* Promyelocytic leukemia nuclear bodies behave as DNA damage sensors whose response to DNA double-strand breaks is regulated by NBS1 and the kinases ATM, Chk2, and ATR. *J Cell Biol* 2006; **175**: 55–66.
23. Xu ZX, Timanova-Atanasova A, Zhao RX, Chang KS. PML colocalizes with and stabilizes the DNA damage response protein TopBP1. *Mol Cell Biol* 2003; **23**: 4247–4256.
24. Bekker-Jensen S, Lukas C, Kitagawa R, Melander F, Kastan MB, Bartek J *et al.* Spatial organization of the mammalian genome surveillance machinery in response to DNA strand breaks. *J Cell Biol* 2006; **173**: 195–206.
25. Stagno D'Alcontres M, Mendez-Bermudez A, Foxon J, Royle NJ, Salomoni P. Lack of TRF2 in ALT cells causes PML-dependent p53 activation and loss od telomeric DNA. *J Cell Biol* 2007; **179**: 855–867.
26. Salomoni P, Pandolfi PP. The role of PML in tumor suppression. *Cell* 2002; **108**: 165–170.
27. Takahashi Y, Lallemand-Breitenbach V, Zhu J, de The H. PML nuclear bodies and apoptosis. *Oncogene* 2004; **23**: 2819–2824.
28. Wiley CA, Schrier RD, Nelson JA, Lampert PW, Oldstone MB. Cellular localization of human immunodeficiency virus infection within the brains of acquired immune deficiency syndrome patients. *Proc Natl Acad Sci USA* 1986; **83**: 7089–7093.
29. Lum JJ, Cohen OJ, Nie Z, Weaver JG, Gomez TS, Yao XJ *et al.* Vpr R77Q is associated with long-term nonprogressive HIV infection and impaired induction of apoptosis. *J Clin Invest* 2003; **111**: 1547–1554.
30. Turelli P, Doucas V, Craig E, Mangeat B, Klages N, Evans R *et al.* Cytoplasmic recruitment of INI1 and PML on incoming HIV preintegration complexes: interference with early steps of viral replication. *Mol Cell* 2001; **7**: 1245–1254.
31. Bernardi R, Pandolfi PP. Role of PML and the PML-nuclear body in the control of programmed cell death. *Oncogene* 2003; **22**: 9048–9057.
32. Castedo M, Perfettini JL, Roumier T, Yakushijin K, Horne D, Medema R *et al.* The cell cycle checkpoint kinase Chk2 is a negative regulator of mitotic catastrophe. *Oncogene* 2004; **23**: 4353–4361.
33. Bartek J, Lukas J. DNA damage checkpoints: from initiation to recovery or adaptation. *Curr Opin Cell Biol* 2007; **19**: 238–245.
34. Bernardi R, Scaglioni PP, Bergmann S, Horn HF, Vousden KH, Pandolfi PP. PML regulates p53 stability by sequestering Mdm2 to the nucleolus. *Nat Cell Biol* 2004; **6**: 665–672.
35. Moller A, Sirma H, Hofmann TG, Rueffer S, Klimczak E, Droge W *et al.* PML is required for homeodomain-interacting protein kinase 2 (HIPK2)-mediated p53 phosphorylation and cell cycle arrest but is dispensable for the formation of HIPK domains. *Cancer Res* 2003; **63**: 4310–4314.

36. Fogal V, Gostissa M, Sandy P, Zacchi P, Sternsdorf T, Jensen K *et al.* Regulation of p53 activity in nuclear bodies by a specific PML isoform. *EMBO J* 2000; **19**: 6185–6195.
37. Zhu H, Wu L, Maki CG. MDM2 and promyelocytic leukemia antagonize each other through their direct interaction with p53. *J Biol Chem* 2003; **278**: 49286–49292.
38. Bleiber G, May M, Martinez R, Meylan P, Ott J, Beckmann JS *et al.* Use of a combined *ex vivo*/*in vivo* population approach for screening of human genes involved in the human immunodeficiency virus type 1 life cycle for variants influencing disease progression. *J Virol* 2005; **79**: 12674–12680.
39. Naldini L, Blömer U, Gallay P, Ory D, Mulligan R, Gage FH *et al. In vivo* gene delivery and stable transduction of nondividing cells by a lentiviral vector. *Science* 1996; **272**: 263–267.
40. Zhou N, Xiao H, Li TK, Nur EKA, Liu LF. DNA damage-mediated apoptosis induced by selenium compounds. *J Biol Chem* 2003; **278**: 29532–29537.

Supplementary Information accompanies the paper on Cell Death and Differentiation website (http://www.nature.com/cdd)